

Abstract

It is important to detect and remove artifacts from fMRI data. However, the sheer volume of data collected for fMRI precludes visually inspecting all the data for artifacts. This suggests a need for tools that will robustly and automatically find artifacts without generating many false positives. To this end, we have developed an algorithm to detect fMRI artifacts that originate from the scanner (i.e., "k-space spikes"). It operates on reconstructed images (not k-space data), is computationally efficient and robustly rejects artifacts from motion or other non-spike events. We have been using this tool as part of our quality assurance program in the Functional Imaging Research in Schizophrenia Testbed Biomedical Information Research Network (FBIRN), an NIH-NCRR initiative in which twelve collaborating sites contribute fMRI data.

Introduction

It is important to detect artifacts from fMRI data, not only so that they do not contaminate downstream processing but also to allow researchers to alter the way the data are collected to avoid the artifacts in the first place. Thus, it is also important to determine not just that an artifact is there, but also the source of the artifact. One such source is a "k-space spike", i.e., a transitory event that happens during the acquisition that causes a large change at a few isolated points in k-space. We distinguish this type of artifact from motion because the mitigation is different. If artifacts are being caused by motion, then the fix is better head restraint, better subject training, etc. On the other hand, k-space spikes are usually caused by some type of scanner hardware malfunction, e.g., an electrical discharge, loose hardware, or "dropped" images, and so it is important for all the users of the scanner that these problems be quickly isolated and fixed. In either case, it is also important that artifacts be detected in contaminated data so that they can be removed prior to processing. Given the sheer size of the data involved, it is impractical to manually inspect each image that comes off the scanner, and so automatic detection is needed.

Background

Automatic artifact detection has been studied by several other groups. Goldfarb and Schmitt, 1996, and Zhang, et al, 2001 examined the raw k-space data for signal changes faster than one would expect from a typical gradient echo. Others (AFNI 3dToutcount, afni.nimh.nih.gov/afni; Luo and Nichols, 2003; Mazaika, et al, 2005) have looked for outliers in the functional time series. The raw k-space methods can be inconvenient as that data is often unavailable off the scanner. k-space spikes are hard to distinguish from motion artifacts in simple outlier counts, and k-space spikes may be lost in whole-brain measures because the spikes tend to only contaminate a single slice.

Methods

One of the differences between a spike artifact and a motion artifact is in the nature of their generation. A spike is fairly rare and is likely to affect only one slice of a given time point whereas motion will likely affect all slices. We exploit this fact in our algorithm by measuring how one slice is different than the other slices. The algorithm is simple:

1. Remove mean and temporal trend from each voxel.
2. Compute temporal Z-score for each voxel.
3. Average the absolute Z-score (AAZ) within each slice and time point separately. This gives a matrix with number of rows equal to the number of slices (nSlices) and number of columns equal to the number of time points (nFrames).
4. Compute new Z-scores using a jackknife across the slices (JKZ). For a given time point, remove one of the slices, compute the average and standard deviation of the AAZ across the remaining slices. Use these two numbers to compute a Z for the slice left out (this is the JKZ). The final Spike Measure is the absolute value of the JKZ (AJKZ). Repeat for all slices (this gives a new nSlices-by-nFrames matrix (see Figure 8)). This procedure tends to remove components that are common across slices and so rejects motion.

As part of the FBIRN Phase I data acquisition, five subjects were scanned twice at each of the ten participating sites (see Figure 2). The scanners were Siemens, GE, and Picker with field strengths of 1.5, 3, and 4T acquiring data with both EPI and spiral trajectories. Each visit consisted of 10 runs for a total of 1000 4D data sets. Each data set was 64x64x35 (3.43x3.43x4mm³) with number of time points ranging from 85 to 144. The TR was 3 sec. There were several experimental protocols: Sternberg item recognition, auditory oddball, sensory-motor, breathhold, and rest. Subjects heads were restrained using a bite-bar. The data and a full description can be found at www.nbirn.net/Resources/Downloads/fBIRN_PhaseI/index.htm.

Results

This algorithm was applied to all of the FBIRN Phase I 4D data sets. Each 4D data set took about 20 sec to run. The distribution of the AJKZ measure across all sites is shown in Figure 1. The vast majority have scores less than 20. We examined the images in the 20-50 range for the telltale signs of k-space spikes and found that AJKZ=25 seemed to be a good threshold for detecting true spikes. Figure 2 shows the number of 4D data sets with spikes according to this measure as a function of scanner. A surprisingly large number of data sets were found to have spikes. However, while all spikes are harmful to functional analysis, it should be pointed out that not all spikes are catastrophic. This method is sensitive enough to find even these subtle spikes.

One of the data sets that exceeded threshold (Stanford, Subject 104, Visit 2, Run 9) was chosen for a more careful analysis. This data set had an AJKZ measure of 29 in slice 28 at time point 25. The unprocessed image show in Figure 3A does not really show any signs of corruption. However, when the mean image is subtracted (Figure 3B), the checkerboard pattern of a spike emerges.

The average within-brain time course (expressed as the absolute z score) is shown in Figure 4. This measure is often suggested for quality control. As can be seen, this measure completely misses the spike. Figure 4 shows the result of AFNI's 3dToutcount. Again, there is nothing about time point 25 to distinguish it from the rest. Figure 6 shows the normalized motion correction plots (AFNI 3dvolreg). Again, there is nothing to suggest anything special about time point 25. Comparison with Figure 5 shows that some of the spikes detected by 3dToutcount are related to motion. Figure 7 shows a plot of the AJKZ spike measure for each slice. As can be seen, time point 25 of slice 28 clearly jumps out where as the other slices and time points have scores more than 30% less. Figure 8 is the same data as that in Figure 7 but rendered as an image to clearly show all slices and time points. The spike (red square at slice 28, time point 25) is easily distinguished.

Conclusions

We have presented an algorithm for detecting k-space spike artifacts in fMRI while rejecting artifacts due to motion. The algorithm is simple to implement and fast to run. It does not require knowledge about the experimental protocol nor does it require access to the original k-space data. We ran it on 1000 4D data sets and found that it could detect even subtle spikes. Whole-brain methods such as mean time course z-score and outlier counts can miss these spikes entirely because they get washed out by noise from the rest of the brain. This software is in regular use by the FBIRN as part of its suite of quality assurance tools. It is also distributed with FreeSurfer (surfer.nmr.mgh.harvard.edu). An SPM toolbox that implements this spike detector is also available at www.cogsci.ucsd.edu/~nwhite/dSPIKES.html.

This poster is available at www.nmr.mgh.harvard.edu/~greve/hbm06-spike-poster.ppt.

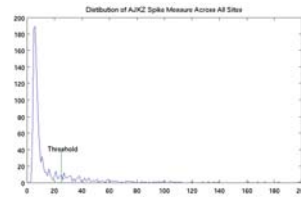


Figure 1: Distribution of AJKZ Spike Measurement over 1000 data sets. The threshold for declaring a spike was set at 25.

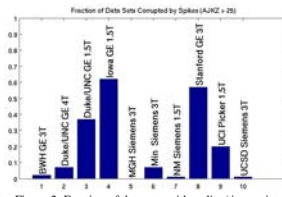


Figure 2: Fraction of data sets with a slice/time point with a spike measure that exceeded threshold.

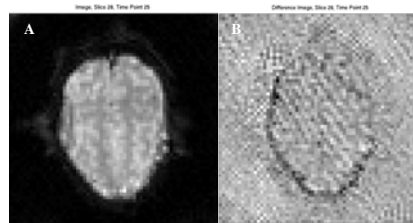


Figure 3: Data set from Stanford, Subject 104, Visit 2, Run 9 (Rest), Slice 28, Time Point 25. Spike Measure = 29. A: Intensity image. The spike is not apparent. B: Difference image shows checkerboard pattern of a spike. Figures 4-8 refer to the full 4D data set for this run.

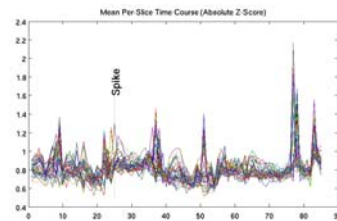


Figure 4: In-brain mean per-slice time course expressed as a z-score for the data set in Figure 3. The spiked time point is barely distinguishable. Prominent peaks seen to be related to motion (see Figure 6) which produce peaks in all 35 slices. Compare to Figure 7.

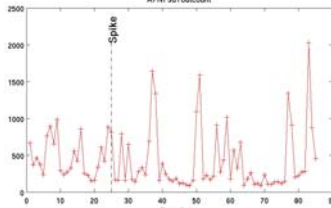


Figure 5: Result of AFNI's 3dToutcount for the data in Figure 3. The presence of the spike is not detectable. Other outliers appear to be motion related (see Figure 6).

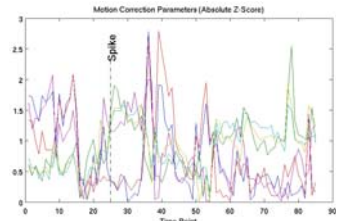


Figure 6: Normalized motion correction parameters from AFNI's 3dvolreg. The presence of the spike is not detectable. Motion appears to be the reason for the outliers in Figures 4 and 5.

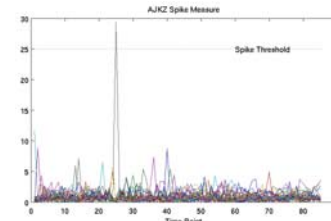


Figure 7: Plot of the AJKZ Spike Measure for all 35 slices. The spiked slice clearly stands out, and the motion outliers in Figures 4 and 5 are suppressed.

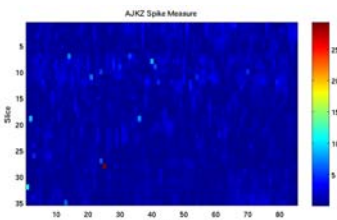


Figure 8: AJKZ Spike Measure for all slices and time points displayed as an image. This is the same data as that in Figure 7. The spike clearly stands out as the red square at slice 28, time point 25.

References

- Goldfarb and Schmitt, 1996. A robust method to remove spike artifacts through HPF post-processing. Proc of ISMRM, NY,NY, p1656.
Zhang, et al, 2001. Elimination of k-space spikes in fMRI data. Mag Res Img, 19, 1037-1041.
Luo and Nichols, 2003. Diagnosis and exploration of massively univariate neuroimaging models. NeuroImage, 19, 1014-1032.
Mazaika, et al, 2005. Detection and repair of transient artifacts in fMRI data. Proc of HBM, Toronto, CA. AFNI, afni.nimh.nih.gov/afni. 3dToutcount, 3dvolreg, 3dSpike.

Acknowledgments: Support for this research was provided in part by the National Center for Research Resources (P41-RR14075, R01-RR16594-01A1) and the NCRR BIRN Morphometric Project BIRN002, U24-RR021382), the National Institute for Biomedical Imaging and Bioengineering (R01-EB001550) as well as the Mental Illness and Neuroscience Discovery (MIND) Institute. This research was supported by a grant (#1 U24-RR021992) to the Functional Imaging Biomedical Informatics Research Network (FBIRN, www.nbirn.net), that is funded by the National Center for Research Resources (NCRR) at the National Institutes of Health (NIH).